CrossMark

RESEARCH ARTICLE

S- to N-Palmitoyl Transfer During Proteomic Sample Preparation

Yuhuan Ji,[1,2] Markus M. Bachschmid,[3] Catherine E. Costello,[1,2] Cheng Lin[1,2]

[1]Center for Biomedical Mass Spectrometry, Boston University School of Medicine, Boston, MA 02118, USA
[2]Department of Biochemistry, Boston University School of Medicine, Boston, MA 02118, USA
[3]Cardiovascular Proteomics Center and Vascular Biology Section, Department of Medicine,
Boston University School of Medicine, Boston, MA 02118, USA

Intermolecular S- to N-palmitoyl transfer
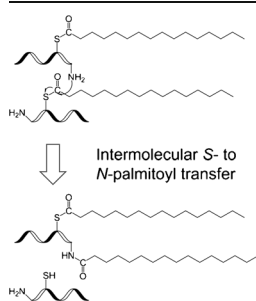
Abstract. N-palmitoylation has been reported in a number of proteins and suggested to play an important role in protein localization and functions. However, it remains unclear whether N-palmitoylation is a direct enzyme-catalyzed process, or results from intramolecular S- to N-palmitoyl transfer. Here, using the S-palmitoyl peptide standard, GC$_{palm}$LGNAK, as the model system, we observed palmitoyl migration from the cysteine residue to either the peptide N-terminus or the lysine side chain during incubation in both neutral and slightly basic buffers commonly used in proteomic sample preparation. Palmitoyl transfer can take place either intra- or intermolecularly, with the peptide N-terminus being the preferred migration site, presumably because of its lower basicity. The extent of intramolecular palmitoyl migration was low in the system studied, as it required the formation of an entropically unfavored macrocycle intermediate. Intermolecular palmitoyl transfer, however, remained a tangible problem, and may lead to erroneous reporting of in vivo N-palmitoylation. It was found that addition of the MS-compatible detergent RapiGest could significantly inhibit intermolecular palmitoyl transfer, as well as thioester hydrolysis and DTT-induced thioester cleavage. Finally, palmitoyl transfer from the cysteine residue to the peptide N-terminus can also occur in the gas phase, during collision-induced dissociation, and result in false identification of N-palmitoylation. Therefore, one must be careful with both sample preparation and interpretation of tandem mass spectra in the study of N-palmitoylation.

Keywords: Palmitoylation, Collision-induced dissociation, Electron transfer dissociation, LC-MS/MS, Peptide fragmentation

Introduction

Protein palmitoylation results from the covalent attachment of a palmitate to amino acid residues. S-palmitoylation is the major form of palmitoylation, where the palmitate is attached to the cysteine sulfhydryl group via a labile thioester linkage (Scheme 1a). S-palmitoylation is reversible and dynamic, and plays an important regulatory role in protein trafficking, membrane localization, and cellular signaling [1]. A less common form, N-palmitoylation, has also been reported, and this involves palmitoyl attachment to the lysine side chain [2–5] or the protein N-terminus (Scheme 1b, c) [6–10]. Unlike S-palmitoylation, N-palmitoylation is irreversible and not regulated. The biological functions of N-palmitoylation are not well understood, but are believed to derive primarily from its interaction with lipid bilayers. Olsen and Andersen suggested that palmitoylation at the lysine (or tyrosine/threonine) residue of the R peptide of the Moloney murine leukemia virus could play a role in controlling the conformation change of the p15E transmembrane protein and regulating the viral budding process [2]. Hackett et al. reported that adenylate cyclase toxin, a virulence factor responsible for forming hemolytic channels and catalyzing the conversion of ATP to 3',5'-cyclic AMP in host cells, underwent palmitoylation at lysine 983 in the wild type *Bordetella pertussis* strain. In contrast, the cyaC-deficient mutant strain lacking the acyltransferase showed no toxin or hemolytic activity, signifying the importance of lysine palmitoylation for membrane insertion and delivery of the catalytic domain [3]. In vivo N-terminal palmitoylation was

Correspondence to: Cheng Lin; *e-mail:* chenglin@bu.edu

(a)

(b)

(c)
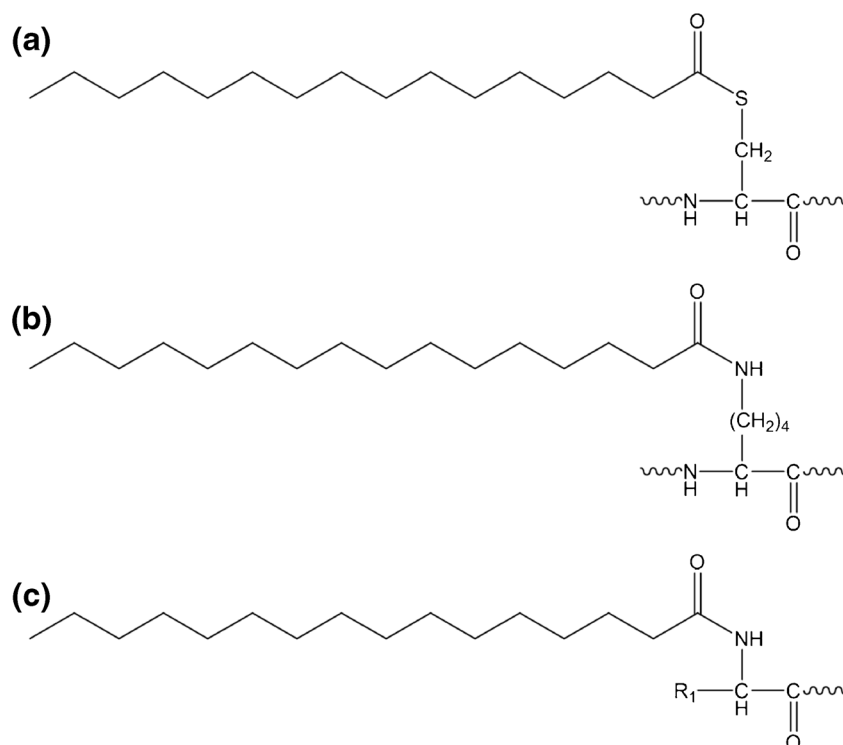
Scheme 1. Chemical structures of *S*-palmitoylation (**a**), and *N*-palmitoylation at the lysine sidechain (**b**), and at the protein N-terminus (**c**)

first detected in human sonic hedgehog (Shh) [6], an extracellular signaling protein that is a key regulator for cell proliferation and differentiation during embryonic development [11]. For Shh, palmitoylation on its N-terminal cysteine is required for its normal distribution and for inducing cell signaling [7, 8]. Another secreted ligand, Spitz, was also found to undergo N-terminal palmitoylation, and this could restrict its diffusion to allow proper local signaling [9]. Recently, Kleuss and Krause reported that the α-subunit of the heterotrimeric G protein (Gα$_s$) is palmitoylated on its N-terminal glycine (Gly^2) [10], in addition to its well-known *S*-palmitoylation site at Cys^3 [12]. Gly^2-palmitoylation appeared to lead to more efficient stimulation of particulate adenylyl cyclases, and this was attributed to its preferential membrane localization. Localization of the palmitoylation site to Gly^2 was confirmed by the observation of a palmitoylated b_I ion in the collision-induced dissociation (CID) spectrum of the tryptic peptide ^{2}G$_{palm}$C$_{IAM}$LGNSK^8.

The mechanism for N-palmitoylation is still under debate. It was originally suggested that N-terminal palmitoylation of Shh is a two-step process involving intramolecular *S*- to *N*-palmitoyl transfer after the initial palmitoyl attachment to the cysteine sulfhydryl group [6]. Consistent with this, Gly^2-palmitoylation was not observed in the Cys^3 mutants of the Gα$_s$ protein. Later, however, Buglino and Resh showed that hedgehog acyltransferase (Hhat) could directly catalyze palmitoyl attachment to the N-terminal amino group of Shh without a thioester intermediate [13]. Interestingly, the three proteins with N-terminal palmitoylation reported to date all contain a cysteine residue either at the N-terminus (Shh and

Spitz), or next to the N-terminus (Gα$_s$). It is unclear whether such proximity of a cysteine residue to the N-terminus is a required motif for the acyltransferase activity, or the evolutionary result to facilitate intramolecular palmitoyl transfer.

Although no explicit studies on *S*- to *N*-palmitoyl migration in peptides have been reported to date, *S*- to *N*-acyl transfer in small model systems has been extensively studied [14–17]. For the series $CH_3COS(CH_2)_nNH_3^+$, at pH < 7, acetyl transfer from sulfur to nitrogen was observed when $n = 2$ or 3, but not for $n \geq 4$ [14]. *S*- to *N*-acyl transfer has also been utilized in protein synthesis by native chemical ligation (NCL) [18]. NCL works effectively when the C-terminal peptide segment of the protein contains a cysteine residue at its N-terminus, thus enabling intramolecular transacylation via an entropically favored five-membered ring intermediate [19]. Similarly, rapid *O*- to *N*-acyl transfer was observed only when the esterified serine residue was present at the N-terminus [20]. The rate of transacylation increases with increasing pH. At pH 8, intramolecular acyl transfer via larger ring intermediates could also take place [14]. As protein characterization often involves sample processing in neutral or slightly basic solutions, it is important to investigate whether *S*- to *N*-palmitoyl migration could occur during sample preparation, when the cysteine residue is not at the N-terminus, and whether this could lead to erroneous reporting of in vivo *N*-palmitoylation.

In this study, an analogue of the N-terminal tryptic peptide from the protein Gα$_s$, ^{2}GCLGNAK^8, was chosen as the model

system to test the palmitoyl migration hypothesis. The serine[7] residue was replaced by an alanine residue to avoid potential interference from *O*-palmitoylation.

Experimental

Materials

Synthetic peptide GCLGNAK was acquired from AnaSpec (San Jose, CA. USA). Palmitoyl chloride, dithiothreitol (DTT), hydroxylamine (HA), and ammonium bicarbonate (ABC) were purchased from Sigma-Aldrich (St. Louis, MO, USA). Trifluoroacetic acid (TFA), formic acid (FA), and iodoacetamide (IAM) were purchased from Pierce (Rockford, IL, USA). RapiGest was obtained from Waters (Milford, MA, USA). 2,5-Dihydroxybenzoic acid (DHB) was obtained from Bruker Daltonics (Billerica, MA, USA). Acetonitrile (ACN) and isopropanol (IPA) were obtained from Burdick and Jackson (Muskegon, MI, USA).

Sample Preparation

Palmitoyl peptide standard GC$_{palm}$LGNAK was produced by incubating GCLGNAK with excess palmitoyl chloride in TFA, followed by C4-RP-HPLC purification on an Agilent 1200 series HPLC system (Agilent Technologies, Santa Clara, CA, USA) as described previously [21]. The incubation typically took place in either 100 mM ABC buffer (pH 8.0) or 50 mM Tris buffer (pH 7.4) at 37 °C for 3 h with or without 0.1% RapiGest. Treatment with DTT (10 mM) was done at 37 °C for 1 h. Treatment with HA (500 mM) was done at room temperature for 1 h. Alkylation by IAM (25 mM) was performed at room temperature for 30 min in dark. The resultant peptides were diluted, co-crystallized with DHB, and analyzed on an ultrafleXtreme MALDI-TOF/TOF instrument (Bruker Daltonics, Billerica, MA, USA). A typical MALDI-TOF mass spectrum was acquired by signal averaging over 4000 laser shots from a Smartbeam-II Nd:YAG laser operating at 355 nm and a repetition rate of 2 kHz. Alternatively, the resultant peptides were desalted by POROS R1 50 and subjected to LC-MS/MS analysis.

Mass Spectrometry Analysis

Offline tandem MS analysis was performed on a solariX hybrid Qh-Fourier transform ion cyclotron resonance mass spectrometer (Bruker Daltonics, Bremen, Germany). Online HPLC-MS/MS analysis was performed on an LTQ-Orbitrap XL instrument (Thermo Fisher Scientific, San Jose, CA, USA) equipped with a nanoAcquity UPLC (Waters, Milford, MA, USA) mounted with a BEH300 C4 column (150 μm i.d. × 10 mm, 1.7 μm, Waters). Mobile phase A consisted of 5:95 ACN/water with 0.1% FA and mobile phase B consisted of 95:5 ACN/water with 0.1% FA. Samples were loaded onto C4-UPLC at 20% B at a flow rate of 0.5 μL/min. The gradient was held at 20% B for 15 min, followed by a ramp to 100% B over 40 min and then held at 100% B for 5 min. It was then ramped to 20%

B over 2 min, and held at 20% B for 25 min for column re-equilibration. Data-dependent acquisition was performed by switching between the MS scan (r = 60,000 @ *m/z* 400) and MS/MS events (r = 30,000 @ *m/z* 400) with an inclusion list of peptides of interest. The isolation window was ±3 *m/z*. The normalized collision energy was set at 35% for CID. Electron transfer dissociation (ETD) reaction time was set at 80 ms with supplemental activation set at 15.

UV Monitoring of S-Palmitoyl Peptides

The kinetics of de-*S*-palmitoylation due to thioester hydrolysis or *S*- to *N*-palmitoyl migration was studied by monitoring the UV absorption of the thioester functional group at λ = 230 nm, measured by an Agilent Cary 60 UV-Vis spectrophotometer (Agilent Technologies, Santa Clara, CA, USA). The UV-Vis absorption of the palmitoyl peptide standard GC$_{palm}$LGNAK was monitored for 3 h following its incubation in 50 mM Tris buffer with or without the presence of 0.1% RapiGest at 37 °C.

Results and Discussion

Preparation of the S-Palmitoyl Peptide GC$_{palm}$LGNAK

Reliable investigation of the *S*- to *N*-palmitoyl migration requires the use of a pure *S*-palmitoyl peptide standard. In vitro palmitoylation with palmitoyl chloride in TFA should produce only *S*- and *O*-palmitoylation, but not *N*-palmitoylation, since the amino and guanidino groups would be protonated in acidic solution and lose their nucleophilic property. Incubation of the peptide standard, GCLGNAK, with palmitoyl chloride in TFA produced a singly palmitoylated peptide, (GCLGNAK)$_{palm}$, as evidenced by the 238.23-Da mass shift in its MALDI-TOF mass spectrum (Supporting Figure S1a, b). HA/IAM treatment of the HPLC-purified peptide (GCLGNAK)$_{palm}$ led to complete palmitoyl loss (Supporting Figure S1c), suggesting that all palmitoyl peptides existed in the form of GC$_{palm}$LGNAK, where the palmitoyl group was connected to the cysteine residue via a thioester linkage, as HA should selectively remove *S*-palmitoylation [22, 23] but not *N*-palmitoylation [24].

Intermolecular Palmitoyl Migration

After a 3-h incubation at 37 °C in either 100 mM ABC buffer (pH 8.0) or 50 mM Tris buffer (pH 7.4), GC$_{palm}$LGNAK gave rise to a mixture of peptides, containing zero, one, or two palmitoyl groups (Figure 1a, b). The presence of a doubly palmitoylated peptide is indicative of the occurrence of in vitro palmitoyl transfer between two palmitoyl peptides. Intermolecular palmitoyl transfer was also observed following incubation of other *S*-palmitoyl peptides (Supporting Figure S2). DTT treatment of the resultant peptide mixture following incubation in ABC buffer produced not only a peptide with no palmitoylation, but also a singly palmitoylated peptide (Supporting Figure S3b), which could be further alkylated by iodoacetamide (Supporting Figure S3c). Thus,
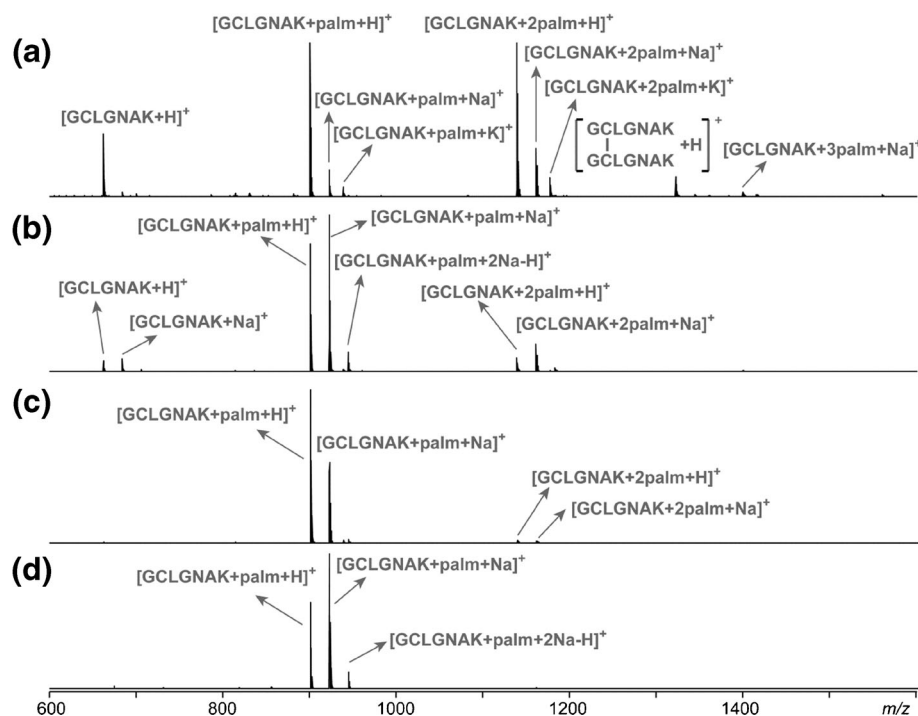
Figure 1. MALDI-TOF mass spectra of the *S*-palmitoyl peptide standard, GC$_{palm}$LGNAK, after incubation (**a**) in 100 mM ABC buffer, (**b**) in 50 mM Tris buffer, (**c**) in 100 mM ABC buffer with 0.1% RapiGest, and (**d**) in 50 mM Tris buffer with 0.1% RapiGest

the remaining palmitoyl group was not on the cysteine side chain. Tandem MS analysis of the doubly charged peptide (GC$_{IAM}$LGNAK)$_{palm}$ revealed the presence of two isomeric species with the palmitoyl group residing either at the N-terminus or on the lysine side chain, based on the observation of a b_2 (palm + IAM) ion and a y_1 (palm) ion in the CID spectrum (Supporting Figure S4).

In neutral or slightly basic solutions, hydrolysis of *S*-palmitoyl peptides should produce primarily palmitate ions (pKa of palmitic acid is 4.78), which are not reactive towards amino groups. Thus, intermolecular *S*- to *N*-palmitoyl transfer must have occurred directly between two palmitoyl peptides without palmitoyl release into the solution, and this would require that the palmitoyl group on one peptide be in the vicinity of the amino group on the other peptide. In support of this hypothesis, a 3-h co-incubation of the peptides GC$_{palm}$LGNAK and GC$_{IAM}$LGNAK in the 100 mM ABC buffer at 37 °C led to intermolecular palmitoyl transfer only between two palmitoyl peptides, but not from a palmitoyl peptide to an IAM-labeled peptide, as no (GC$_{IAM}$LGNAK)$_{palm}$ peptide was observed (Supporting Figure S5). This preference may be attributed to the aggregation of palmitoyl peptides in aqueous solutions because of the hydrophobic interaction between their palmitoyl groups. Such interaction was lacking between an IAM-labeled peptide and a palmitoyl peptide.

If the intermolecular *S*- to *N*-palmitoyl migration was facilitated by the aggregation of palmitoyl peptides, it could be suppressed by disrupting their hydrophobic interaction. To test this hypothesis, GC$_{palm}$LGNAK was incubated in either 100 mM ABC buffer or 50 mM Tris buffer with 0.1% RapiGest (structure shown in Scheme 2), an MS-compatible detergent

commonly used to solubilize proteins and to prevent protein/peptide aggregation. The MALDI mass spectrum remained largely unchanged after 3-h incubation at 37 °C, although a very low level of doubly palmitoylated peptide was observed (Figure 1c, d). Therefore, it seems that the presence of detergents can significantly reduce the extent of intermolecular palmitoyl transfer.

Intermolecular Versus Intramolecular Palmitoyl Migration

Although the MALDI-TOF MS analysis provided solid evidence for the occurrence of intermolecular palmitoyl migration, it could not provide information on whether the palmitoyl group was transferred to the peptide N-terminus or the lysine side chain. Neither could it suggest whether intramolecular migration took place since it is not possible to differentiate among the three palmitoyl peptides, GC$_{palm}$LGNAK, G$_{palm}$CLGNAK, and GCLGNAK$_{palm}$, based solely on their *m/z* values. LC-MS/MS analysis was therefore performed to distinguish and determine the relative abundances of various palmitoyl peptide isomers, as isomeric palmitoyl peptides can
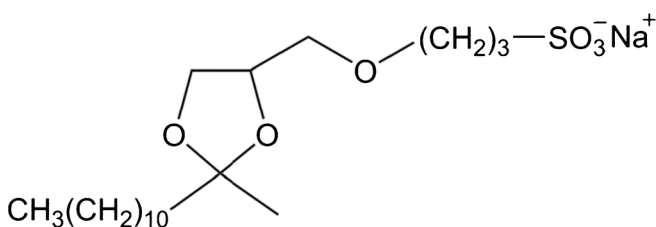
Scheme 2. Chemical structure of RapiGest

be separated by reversed phase HPLC [20], and the palmitoylation site can be localized by tandem MS analysis. All samples were analyzed by online-C4-UPLC-MS/MS analysis on an LTQ-Orbitrap XL instrument with equal sample loading amounts. Figure 2 shows the base peak chromatogram (BPC) and the extracted ion chromatograms (EICs) of various forms of peptides identified after a 3-h incubation of $GC_{palm}LGNAK$ in the Tris buffer. The palmitoylation sites on various peptides were determined based on their tandem mass spectra and will be discussed later. Note that the depalmitoylated peptide, GCLGNAK, observed in the MALDI-TOF mass spectra, was not detected by LC-MS/MS because it is very hydrophilic and would have been removed during the desalting step. EIC of $[GCLGNAK + palm + 2H]^{2+}$ (*m/z* 450.783) contains a single peak (Figure 2b), and it is assigned as $GC_{palm}LGNAK$ based on the similarity of its retention time (RT = 40.8 min) and fragmentation pattern to those of the $GC_{palm}LGNAK$ standard. Meanwhile, EIC of $[GCLGNAK + 2palm + 2H]^{2+}$ (*m/z* 569.898) (Figure 2c) contains two peaks with baseline separation, and these two isomers are later identified as $GC_{palm}LGNAK_{palm}$ (RT = 51.9 min) and $G_{palm}C_{palm}LGNAK$ (RT = 53.2 min). Another pair of isomeric peptides (*m/z* 899.551) was also observed in very low abundance; they correspond to the disulfide-bonded homo-dimer of $GCLGNAK_{palm}$ (RT = 47.25 min) and of $G_{palm}CLGNAK$ (RT = 47.76 min) (Figure 2d), presumably formed after intramolecular palmitoyl transfer. These dimers were not observed in the MALDI-TOF mass spectra.

The BPC and EICs of various forms of peptides produced following a 3-h incubation of $GC_{palm}LGNAK$ in the Tris buffer with 0.1% RapiGest are shown in Supporting Figure S6. The effect of RapiGest on *S*- to *N*-palmitoyl migration can be evaluated by comparing the relative abundances of the various peptides that resulted from incubation of $GC_{palm}LGNAK$ in the Tris and Tris-RapiGest buffers from the LC-MS/MS data. The absolute ion abundance of each peptide was measured as the

sum of the charge-state normalized integrated peak areas of all observed charge states in their respective EICs and presented in a bar graph (Figure 3). Each data set was derived from five experimental repeats with the same loading amount. The average ion abundance of each peptide and its relative ratio between the two incubation conditions are listed in Supporting Table S1. The N-terminus appeared to be the favored palmitoyl migration site. This is consistent with the fact that the N-terminal amino group is less basic than the lysine sidechain $[pKa_3(Lys) = 10.53$, and $pKa_2(Gly) = 9.60]$, and thus more likely to exist in its unprotonated (and reactive) form in the Tris buffer (pH = 7.4). Addition of RapiGest led to a significant decrease in the level of $GC_{palm}LGNAK_{palm}$ and $G_{palm}C_{palm}LGNAK$, and a moderate increase in the level of disulfide-bonded homodimers, especially the $G_{palm}CLGNAK$ dimer. This is understandable, as solvation of the hydrophobic palmitoyl group by the RapiGest should inhibit intermolecular palmitoyl migration and may facilitate intramolecular palmitoyl migration, with preference to the N-terminus because of its proximity to the palmitoylated cysteine residue. It is, however, not possible to determine the percentage of the $GC_{palm}LGNAK$ peptides that underwent inter- or intra-molecular palmitoyl migration based on the LC-MS/MS result, since the resultant peptides have different ionization efficiencies.

Stabilization of S-Palmitoyl Groups by RapiGest

The thioester group has a strong UV absorption at 230 nm with an extinction coefficient (ε) of 4300 M^{-1} cm^{-1} compared with that of the amide group ($\varepsilon = 122$ M^{-1} cm^{-1}) [16]. Thus, the change in the *S*-palmitoyl content, or concentration (*c*), under various incubation conditions can be studied by monitoring the UV absorbance (*A*) at 230 nm, according to the Lambert-Beer Law: $A = \varepsilon c L$, where *L* is the light path length. Supporting Figure S7a shows that the UV absorbance of $GC_{palm}LGNAK$ was reduced by nearly half following 3-h incubation in the Tris

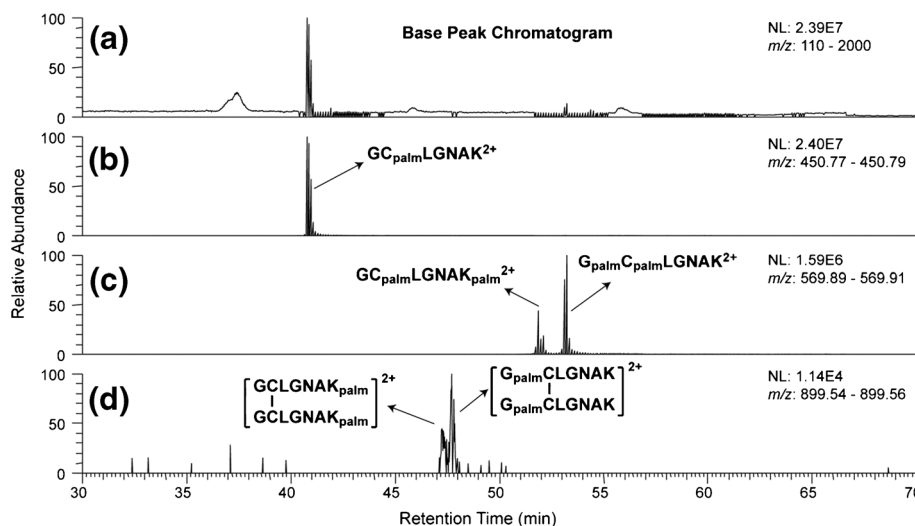

Figure 2. (a) The base peak chromatogram of $GC_{palm}LGNAK$ after incubation in 50 mM Tris buffer at 37 °C for 3 h; (b) (c) (d) the extracted ion chromatograms of various modified forms of GCLGNAK

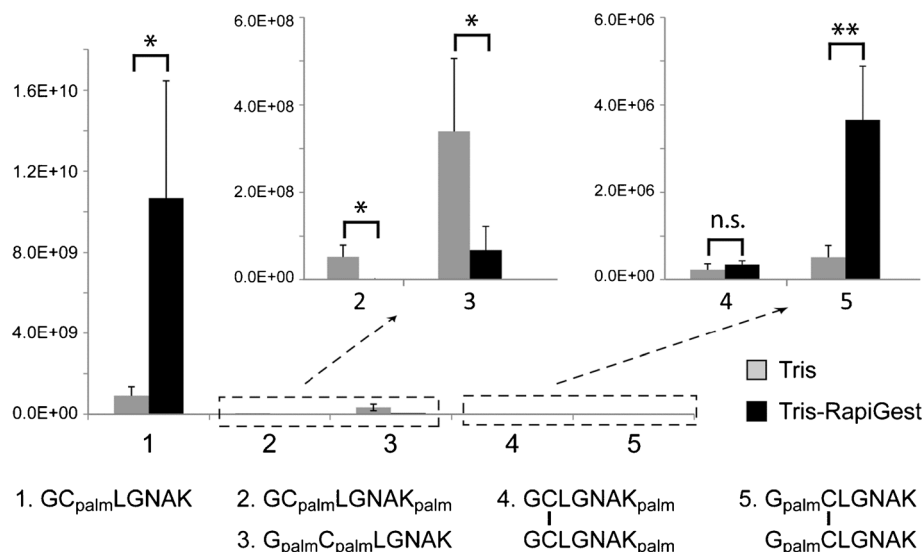**Figure 3.** Comparison of the ion abundances of $GC_{palm}LGNAK$-derived peptides after 3-h incubation in 50 mM Tris buffer in the absence or presence of 0.1% RapiGest. Unpaired *t*-test, standard deviation, $n = 5$, * $p < 0.05$, ** $p < 0.01$

buffer, indicating a significant loss of *S*-palmitoylation. This is in stark contrast to the previous observation that the *S*-palmitoyl group in several palmitoyl peptide standards was stable in the neutral Tris buffer [21]. Meanwhile, *S*-palmitoyl loss was barely detectable when RapiGest was added to the incubation buffer (Supporting Figure S7b), and thus the abundance ratio of $GC_{palm}LGNAK$ in the Tris and in the Tris-RapiGest samples can be used to estimate the extent of palmitoyl loss during incubation in the Tris buffer. If the 12-fold drop in ion abundance in the Tris sample (Supporting Table S1) had all been caused by intermolecular palmitoyl transfer, the UV absorbance would have dropped by about 46% because half of the products still contained the thioester chromophore. Intramolecular palmitoyl transfer and/or thioester hydrolysis may account for the slightly larger drop in the UV absorbance. Nonetheless, it appeared that intermolecular palmitoyl transfer was the main contributor to the initial drop in the *S*-palmitoyl content, whereas thioester hydrolysis of the di-palmitoylated peptide products may lead to further drop in the UV absorbance at later time points. Considering that ion abundance of the disulfide-bonded dimers of *N*-palmitoylated peptides in the Tris sample is even lower than that in the Tris-RapiGest sample, the negligible decay of UV absorbance at 230 nm over 3-h incubation in the Tris-RapiGest buffer suggests that intramolecular palmitoyl transfer is a very slow process for this peptide, where the cysteine residue is only one residue away from the N-terminus.

The stabilizing effect of RapiGest upon *S*-palmitoylation was further investigated by incubating the three previously studied palmitoyl peptide standards in the presence of DTT. All three palmitoyl peptides underwent severe palmitoyl loss when DTT was added to the neutral Tris buffer, whereas addition of RapiGest greatly decelerated the DTT-induced depalmitoylation process in all cases, as shown in Figure 4. We suggest that the hydrophobic alkyl chain of the palmitoyl group can either insert into the RapiGest micelle or aggregate

with the RapiGest molecules, and such interaction would shield the thioester group from nucleophilic attacks by water, DTT, or other nucleophilic groups, including the amino group at the protein N-terminus or the lysine side-chain, thus stabilizing the *S*-palmitoylation.

Tandem MS Analysis of Palmitoyl Peptide Isomers

In proteomic studies, tandem MS is often used for characterization of post-translational modifications (PTMs). Successful PTM localization requires PTM retention on its original site. However, CID can lead to loss of labile PTMs, such as sulfation and *O*-glycosylation, thus preventing accurate PTM localization. Additionally, PTM relocation has been observed during CID of phosphotyrosine-containing peptide monoanions [25], although another study suggested that such relocation of phosphate group was minimal during CID of both tryptic and Lys-N generated peptide cations [26].

Here, we first investigated the LC-MS/MS behaviors of the three singly palmitoyl peptide isomers. The EIC of the *S*-palmitoyl peptide standard $GC_{palm}LGNAK$ contains a single peak (Figure 5a), with the doubly charged ions as the dominant species in its mass spectrum (Figure 5c). Incubation in 100 mM ABC buffer followed by DTT treatment produced three peaks in the EIC of the singly palmitoylated species (Figure 5b). The isomer with the shortest retention time was identified as $GC_{palm}LGNAK$, as its retention time, ionization pattern, and CID/ETD spectra are similar to those of the *S*-palmitoyl peptide standard (Figure 6a, Supporting Figure S8a). The isomer with the intermediate retention time was assigned as $GCLGNAK_{palm}$ based on the observation of a series of palmitoylated *y* and *z* ions in its CID/ETD spectra (Figure 6b, Supporting Figure S8b). The isomer with the longest retention time was assigned as $G_{palm}CLGNAK$ based on the presence of a series of palmitoylated *b* and *c* ions in its CID/ETD spectra (Figure 6c, Supporting Figure S7c). Noticeably, $GCLGNAK_{palm}$ and
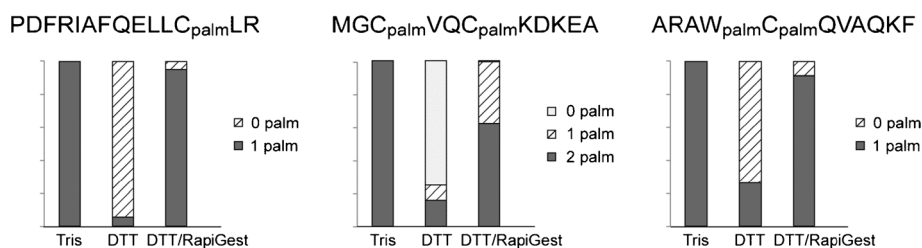
Figure 4. Stability of the three palmitoyl peptide standards, as represented by the relative abundances of the palmitoyl peptides and their various depalmitoylated forms after 1-h incubation in 50 mM Tris, 50 mM Tris/10 mM DTT, and 50 mM Tris/0.1% RapiGest/ 10 mM DTT. All experiments were performed at 37 °C

$G_{palm}CLGNAK$ produced doubly charged precursor ions in much lower abundance than $GC_{palm}LGNAK$ (Figure 5c) because one of the two favored protonation sites was occupied by the transferred palmitoyl group.

As expected, the CID spectrum of $GC_{palm}LGNAK$ (Figure 6a) was characterized by a series of palmitoylated *b* ions (b_2–b_6) and *y*-ions without palmitoylation (y_1, y_2, y_4, and y_5). Surprisingly, a palmitoylated a_1, a palmitoylated b_1 and an unpalmitoylated y_6 ion were also observed in relatively high abundance, although they were supposed to be the diagnostic ions for palmitoylation at the N-terminus. The presence of these ions suggests the occurrence of palmitoyl migration from the cysteine residue to the peptide N-terminus during the CID process. For peptide ions, formation of *b* and *y* ions during CID is believed to be initiated by proton migration from a charged basic site (e.g., the amino group at the N-terminus) to an amide group along the peptide backbone, which not only

(a) $GC_{palm}LGNAK$

(b) $GCLGNAK_{palm}$

$GC_{palm}LGNAK$ $G_{palm}CLGNAK$

(c) $GC_{palm}LGNAK$ $GCLGNAK_{palm}$ $G_{palm}CLGNAK$

$[M+2H]^{2+}$ $[M+H]^+$ $[M+H]^+$

$[M+2H]^{2+}$ $[M+2H]^{2+}$
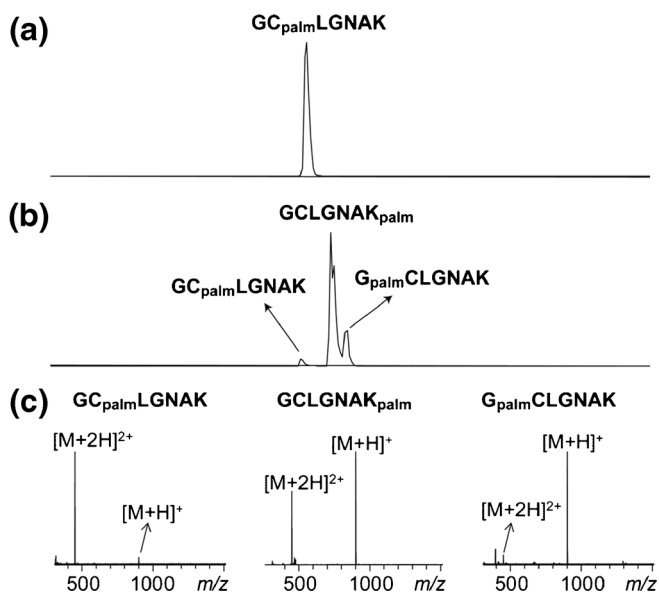
$[M+H]^+$

500 1000 *m/z* 500 1000 *m/z* 500 1000 *m/z*

Figure 5. Integrated EICs of the singly palmitoylated species [GCLGNAK + palm] obtained from the LC-MS analysis of the *S*-palmitoyl peptide standard, $GC_{palm}LGNAK$, (**a**) before and (**b**) after a 3-h incubation in 100 mM ABC buffer at 37 °C followed by DTT reduction. (**c**) Mass spectra of the three isomers. Note that each integrated EIC represents the sum of the singly (*m/z* 450.78) and doubly (*m/z* 900.56) charged species of [GCLGNAK + palm]
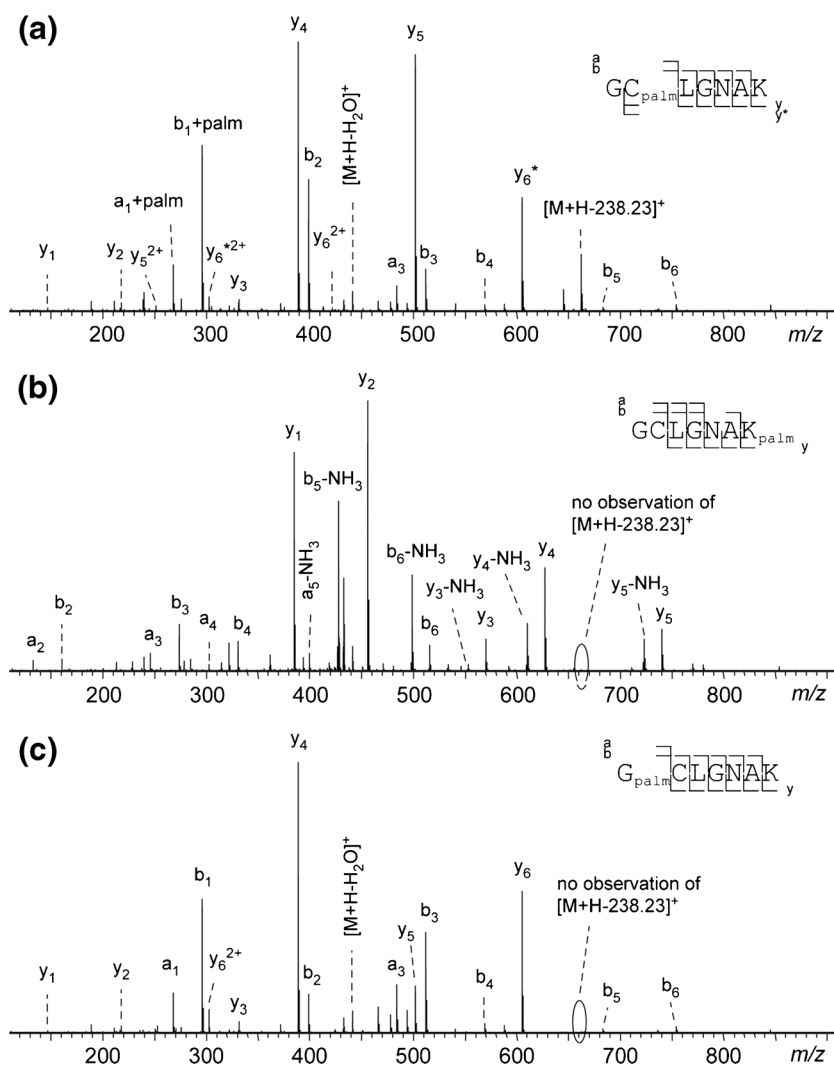
weakens the amide bond but also increases the electrophilicity of the amide carbon. The amide carbon is subsequently attacked by the oxygen from its N-terminal neighboring carbonyl group followed by chemical rearrangement to produce an oxazolone *b* ion and its complementary *y* ion (Supporting Scheme S1) [27]. The b_1 ion cannot be produced via the oxazolone pathway because there is no carbonyl oxygen on the N-terminal side of the first amide group along the peptide backbone. For the peptide $GC_{palm}LGNAK$, however, the carbonyl group of the cysteine thioester undergoes nucleophilic attack by the N-terminal nitrogen during CID, leading to the transfer of the palmitoyl group from the cysteine thiol to the amine at the N-terminus. After migration, the carbonyl oxygen from the palmitoyl group can attack the N-terminal amide carbon to produce a palmitoylated b_1 ion and its complementary unpalmitoylated y_6 ion (Supporting Scheme S2). Because of the palmitoyl migration, CID of $GC_{palm}LGNAK$ generated the same *b*- and *y*-ion series as those of $G_{palm}CLGNAK$ (Figure 6c), but with different ion abundances. A major difference between the CID spectra of these two peptides is the presence of a $[M + H - 238.23]^+$ ion in the $GC_{palm}LGNAK$ spectrum but not in that of $G_{palm}CLGNAK$. The 238.23-Da loss from the precursor ion is characteristic of *S*-palmitoyl peptides, resulting from the loss of a palmitoyl group ($C_{16}H_{30}O$) [21]. On the other hand, the stability of an amide-linked acyl group under CID was previously reported for myristoylated peptides [28]. The absence of palmitoyl loss in CID of the lysine side chain-palmitoylated $GCLGNAK_{palm}$ (Figure 6c) further validates the use of $[M + H - 238.23]^+$ ion for differentiation of *S*- and *N*-palmitoyl peptide isomers.

The lysine palmitoylation in $GCLGNAK_{palm}$ could also be identified by ETD based on the observation of several palmitoylated *z* ions (Supporting Figure S8b). However, it was challenging to use ETD to differentiate $GC_{palm}LGNAK$ and $G_{palm}CLGNAK$, as ETD produced the same backbone fragments from these two isomers (Supporting Figure S8a, c). One of the potential diagnostic ions, c_1, was absent, presumably due to the neutralization of the charge at the N-terminus. The other potential diagnostic ion, the palmitoylated z_6 ion from $GC_{palm}LGNAK$, underwent facile radical-induced side chain loss, producing the same w_6 ion (*m/z* 556.31) as that of $G_{palm}CLGNAK$. However, unlike dissociation of $G_{palm}CLGNAK$, the ETD spectrum of $GC_{palm}LGNAK$ contains two peaks assigned as $[M + 2H - C_{15}H_{31}COHS]^{+\bullet}$ (*m/z*

Figure 6. CID tandem mass spectra of (a) $GC_{palm}LGNAK$, (b) $GCLGNAK_{palm}$, and (c) $G_{palm}CLGNAK$

629.35) and $[M + 2H - NH_3]^{+\bullet}$ (m/z 844.54). The neutral loss of $C_{15}H_{31}COHS$ from the precursor ion was often observed in ECD and ETD of *S*-palmitoyl peptides [21], produced by electron transfer to the protonated carbonyl of the thioester linkage followed by the radical-induced alpha cleavage (Supporting Scheme S3). NH_3 loss from the charge-reduced precursor ions is common in ECD/ETD, and generally does not provide any information for peptide sequencing. However, as the NH_3 loss often originates from the N-terminal amine, the absence of NH_3 loss could suggest a modified N-terminus [29].

The doubly palmitoylated isomers (m/z 569.898) can be similarly discriminated from one another based on their fragmentation behaviors. A 3-h incubation of $GC_{palm}LGNAK$ in the Tris or Tris/RapiGest buffer produced two doubly palmitoylated isomers (Figure 2c, Supporting Figure S6c). The CID spectrum of the isomer that eluted first (RT = 51.9 min) (Supporting Figure S9a) was characterized by a series of palmitoylated *y* ions (y_1, y_2, y_4, and y_5), indicating that the C-terminal lysine was one of the palmitoylation sites. Meanwhile, the presence of a $[M + H - 238.23]^+$ ion indicated that the second palmitoyl group was attached to the cysteine

residue. Thus, the first isomer could be identified as $GC_{palm}LGNAK_{palm}$. The isomer that eluted later (RT = 53.2 min) was similarly identified as $G_{palm}C_{palm}LGNAK$ based on the observation of a $[M + H - 238.23]^+$ ion and a series of *b* ions carrying two palmitoyl groups (b_2–b_6) (Supporting Figure S9b). The CID spectra of the two disulfide-bonded dimers (Figure 2d, Supporting Figure S6d) are shown in Supporting Figure S10; these could be assigned as the homo-dimer of $GCLGNAK_{palm}$ (RT = 47.25 min) and $G_{palm}CLGNAK$ (RT = 47.76 min), based on the characteristic palmitoylated *y* ions and *b* ions, respectively.

Conclusions

Here, using the *S*-palmitoyl peptide standard, $GC_{palm}LGNAK$, as the model system, we observe palmitoyl migration from the cysteine residue to either the peptide N-terminus or the lysine side chain during incubation in both neutral (Tris, pH 7.4) and slightly basic (ABC, pH 8.0) buffers commonly used for proteomic sample preparation. Moreover, a high degree of *S*-

palmitoyl loss was observed in GC$_{palm}$LGNAK, even in the neutral Tris buffer, and we determined that this was primarily caused by intermolecular *S*- to *N*-palmitoyl transfer. On the other hand, intramolecular *S*- to *N*-palmitoyl transfer was insignificant for this peptide, which does not contain an N-terminal cysteine residue. It was found that addition of the MS-compatible detergent RapiGest, at suggested concentration, could significantly inhibit thioester hydrolysis, DTT-induced thioester cleavage, and intermolecular *S*- to *N*-palmitoyl migration. Therefore, RapiGest is recommended during palmitoyl protein/peptide sample preparation. The palmitoylation site(s) in various palmitoyl peptide isomers can be generally determined by tandem MS analysis. However, complications may arise because of the gas-phase transfer of the palmitoyl group from the cysteine residue to the peptide N-terminus during CID, which could lead to false identification of *N*-palmitoylation. One must be careful with sample preparation and interpretation of tandem mass spectra in the study of *N*-palmitoylation.

Acknowledgments

References

1. Smotrys, J.E., Linder, M.E.: Palmitoylation of intracellular signaling proteins: regulation and function. Annu. Rev. Biochem. **73**, 559–587 (2004)
2. Olsen, K.E.P., Andersen, K.B.: Palmitoylation of the intracytoplasmic R peptide of the transmembrane envelope protein in moloney murine leukemia virus. J. Virol. **73**, 8975–8981 (1999)
3. Hackett, M., Guo, L., Shabanowitz, J., Hunt, D., Hewlett, E.: Internal lysine palmitoylation in adenylate cyclase toxin from bordetella pertussis. Science **266**, 433–435 (1994)
4. Fong, K.P., Tang, H.Y., Brown, A.C., Kieba, I.R., Speicher, D.W., Boesze-Battaglia, K., Lally, E.T.: Aggregatibacter actinomycetemcomitans leukotoxin is post-translationally modified by addition of either saturated or hydroxylated fatty acyl chains. Mol. Oral. Microbiol. **26**, 262–276 (2011)
5. Gustafsson, M., Curstedt, T., Jörnvall, H., Johansson, J.: Reverse-phase HPLC of the hydrophobic pulmonary surfactant proteins: detection of a surfactant protein C isoform containing N-epsilon-palmitoyl-lysine. Biochem. J. **326**, 799–806 (1997)
6. Pepinsky, R.B., Zeng, C., Wen, D., Rayhorn, P., Baker, D.P., Williams, K.P., Bixler, S.A., Ambrose, C.M., Garber, E.A., Miatkowski, K., Taylor, F.R., Wang, E.A., Galdes, A.: Identification of a palmitic acid-modified form of human sonic hedgehog. J. Biol. Chem. **273**, 14037–14045 (1998)
7. Chen, M.-H., Li, Y.-J., Kawakami, T., Xu, S.-M., Chuang, P.-T.: Palmitoylation is required for the production of a soluble multimeric

8. Taylor, F.R., Wen, D., Garber, E.A., Carmillo, A.N., Baker, D.P., Arduini, R.M., Williams, K.P., Weinreb, P.H., Rayhorn, P., Hronowski, X., Whitty, A., Day, E.S., Boriack-Sjodin, A., Shapiro, R.I., Galdes, A., Pepinsky, R.B.: Enhanced potency of human sonic hedgehog by hydrophobic modification. Biochemistry **40**, 4359–4371 (2001)
9. Miura, G.I., Buglino, J., Alvarado, D., Lemmon, M.A., Resh, M.D., Treisman, J.E.: Palmitoylation of the EGFR ligand Spitz by rasp increases Spitz activity by restricting its diffusion. Dev. Cell **10**, 167–176 (2006)
10. Kleuss, C., Krause, E.: Gα$_s$ is palmitoylated at the N-terminal glycine. EMBO J. **22**, 826–832 (2003)
11. Ingham, P.W., McMahon, A.P.: Hedgehog signaling in animal development: paradigms and principles. Genes Dev. **15**, 3059–3087 (2001)
12. Linder, M.E., Middleton, P., Hepler, J.R., Taussig, R., Gilman, A.G., Mumby, S.M.: Lipid modifications of G proteins: alpha subunits are palmitoylated. Proc. Natl. Acad. Sci. **90**, 3675–3679 (1993)
13. Buglino, J.A., Resh, M.D.: Hhat is a palmitoylacyltransferase with specificity for *N*-palmitoylation of sonic hedgehog. J. Biol. Chem. **283**, 22076–22088 (2008)
14. Wieland, T., Hornig, H.: S-acylspaltung bei S-acetyl-ω-aminomercaptanen verschiedener Kettenlänge. Justus Liebigs Ann. Chem. **600**, 12–22 (1956)
15. Martin, R.B., Hedrick, R.I.: Intramolecular S-O and S-N acetyl transfer reactions. J. Am. Chem. Soc. **84**, 106–110 (1962)
16. Barnett, R.E., Jencks, W.P.: Diffusion-controlled proton transfer in intramolecular thiol ester aminolysis and thiazoline hydrolysis. J. Am. Chem. Soc. **91**, 2358–2369 (1969)
17. Cuccovia, I.M., Schroeter, E.H., De Baptista, R.C., Chaimovich, H.: Effect of detergents on the S- to N-acyl transfer of S-acyl-β-mercaptoethylamines. J. Org. Chem. **42**, 3400–3403 (1977)
18. Dawson, P., Muir, T., Clark-Lewis, I., Kent, S.: Synthesis of proteins by native chemical ligation. Science **266**, 776–779 (1994)
19. Monbaliu, J.-C.M., Katritzky, A.R.: Recent trends in Cys- and Ser/Thr-based synthetic strategies for the elaboration of peptide constructs. Chem. Commun. **48**, 11601–11622 (2012)
20. Mouls, L., Subra, G., Enjalbal, C., Martinez, J., Aubagnac, J.L.: O–N-Acyl migration in N-terminal serine-containing peptides: mass spectrometric elucidation and subsequent development of site-directed acylation protocols. Tetrahedron Lett. **45**, 1173–1178 (2004)
21. Ji, Y., Leymarie, N., Haeussler, D.J., Bachschmid, M.M., Costello, C.E., Lin, C.: Direct detection of S-palmitoylation by mass spectrometry. Anal. Chem. **85**, 11952–11959 (2013)
22. Tu, Y., Wang, J., Ross, E.M.: Inhibition of brain Gz GAP and other RGS proteins by palmitoylation of G protein α subunits. Science **278**, 1132–1135 (1997)
23. Levental, I., Lingwood, D., Grzybek, M., Coskun, Ü., Simons, K.: Palmitoylation regulates raft affinity for the majority of integral raft proteins. Proc. Natl. Acad. Sci. **107**, 22050–22054 (2010)
24. Resh, M.D.: Targeting protein lipidation in disease. Trends Mol. Med. **18**, 206–214 (2012)
25. Edelson-Averbukh, M., Shevchenko, A., Pipkorn, R., Lehmann, W.D.: Gas-phase intramolecular phosphate shift in phosphotyrosine-containing peptide monoanions. Anal. Chem. **81**, 4369–4381 (2009)
26. Mischerikow, N., Altelaar, A.F.M., Navarro, J.D., Mohammed, S., Heck, A.: Comparative assessment of site assignments in CID and ETD spectra of phosphopeptides discloses limited relocation of phosphate groups. Mol. Cell. Proteom. **9**, 2140–2148 (2010)
27. Wysocki, V.H., Tsaprailis, G., Smith, L.L., Breci, L.A.: Mobile and localized protons: a framework for understanding peptide dissociation. J. Mass Spectrom. **35**, 1399–1406 (2000)
28. Hoffman, M.D., Kast, J.: Mass spectrometric characterization of lipid-modified peptides for the analysis of acylated proteins. J. Mass Spectrom. **41**, 229–241 (2006)
29. Xia, Q., Lee, M., Rose, C., Marsh, A., Hubler, S., Wenger, C., Coon, J.: Characterization and diagnostic value of amino acid side chain neutral losses following electron-transfer dissociation. J. Am. Soc. Mass Spectrom. **22**, 255–264 (2011)